Tampere University

Daria Briukhanova

PLASMONIC NANOANTENNAS ON EPSILON-NEAR-ZERO METAMATERIAL SUBSTRATES

Bachelor of Science thesis
Examiner: Assoc. Prof. Humeyra Caglayan
February 2020

ABSTRACT

Daria Briukhanova: Plasmonic nanoantennas on Epsilon-Near-Zero Metamaterial substrates
Bachelor of Science thesis
Tampere University
International Bachelor's Degree Programme in Science and Engineering
February 2020

The localized surface plasmon resonance (LSPR) is used for light confinement within sub-wavelength scale. The fields are localized and re-directed with the metal nanoantennas. The localization of electric field inside and outside of such a nanoantenna depends upon its shape, the metal, and substrate. Therefore, it is possible to tailor the resonant wavelength by changing the nanoantenna parameters. In this thesis, I have used epsilon-near-zero (ENZ) metamaterial as a substrate to dictate the LSPR of golden (Au) nanodisk (ND) antenna arrays. The hyperbolic metamaterial (HMM), which consists of metal and dielectric alternating layers, designed to have an effective permittivity (epsilon) close to zero. The ENZ substrate with almost zero index slows down the resonance shift of NDs which is known as "pinning effect". I have experimentally demonstrated the pinning effect, by comparing the transmission of ND antennas on glass to the transmission of NDs on HMM with ENZ wavelength at 684 nm. The NDs on HMM substrate have three times less spectral shift compare to the NDs on glass. The robust control of LSPR with ENZ metamaterial substrate can be applied in emission enhancing and beam steering.

Keywords: Localized surface plasmon resonance, epsilon-near-zero metamaterial, hyperbolic metamaterial, pinning effect

ACKNOWLEDGEMENTS

I would like to express my sincere gratitude to Assoc. Prof. Humeyra Caglayan for providing me with the opportunity to join her group. I get inspired everyday working alongside her and our team. I thank her for encouraging me with my work and studies. I could not have envisioned the completion of my thesis without her continuous support and supervision.

I convey my utmost appreciation to Mohsin Habib for being an amazing mentor. His thorough guidance and advice not only made this thesis possible but also made the whole experience truly remarkable. I feel grateful for his effort he put into my work from clarifying difficult concepts to his constructive feedback on my thesis writing.

I would like to thank Dr. Bilge Yildiz Karakul for teaching me how to use simulation software, recommending relevant papers and generally for just being there whenever I needed her guidance. I also thank Dr. Alireza Rahimi Rashed and Nekhel Das for assisting me with confocal microscopy measurements.

Last but not the least, I thank all the staff from the cleanroom, especially Jarno Reuna and Mervi Koskinen for arranging all the training. If not for their profound instructions and suggestions, I would not have managed to overcome all the challenges in the fabrication process.

Tampere, 01.02.2020

Daria Briukhanova

TABLE OF CONTENTS

LIST OF ABBREVIATIONS AND SYMBOLS

SPP	surface plasmon polariton
EM	electromagnetic
LSPR	localized surface plasmon resonance
ENZ	epsilon-near-zero
ITO	indium tin oxide
Al:ZnO	aluminium zinc oxide
Ga:ZnO	gallium zinc oxide
NIR	near-infrared
MIR	mid-infrared
HMM	hyperbolic metamaterial
ND	nanodisk
Au	gold
TiO_2	titanium dioxide
NP	nanoparticle
4H-SiC	silicon carbide
PML	perfect matched layer
Ti	titanium
EBL	electron beam lithography
PMMA	polymethyl methacrylate
SEM	scanning electron microscopy
Al	aluminium

1. INTRODUCTION

Nanophotonics is the study of light matter interaction by the confinement light into small volumes or areas. Recently, the confinement of light is effectively used in optical sensors by providing the identification of small changes and in optical processing and generation of quantum light sources.

Plasmonics is a recently emerged branch of nanophotonics that studies the interaction of light with metals at nanoscale [1]. The surface plasmon polariton (SPP) is a propagating electromagnetic (EM) wave bound between two surfaces of materials (metal and dielectric) with the permittivities of opposite sign. Whereas, the localized surface plasmons resonance (LSPR) is the outcome of a confined surface plasmon, when the light source with comparable wavelength excites the metallic nanoantenna [2]. The LSPR results in a strong electric field across the antenna. The electric filed is localized at the resonance wavelength of nanoantenna, that is governed by the size, shape, material composition, local environment and the substrate [3].

One of the interesting material studied is epsilon-near-zero (ENZ) material. The ENZ materials have real permittivity $Re(\epsilon)$ close to zero for a range of frequencies and very small value of imaginary permittivity $Im(\epsilon)$ [4]. The ENZ effects can be used for enhanced transmission of incident light, decreased phase variation within the substrate and nearly vanishing index of refraction [5]. The ENZ materials were earlier used as a substrate [6] such as indium tin oxide (ITO), aluminium and gallium doped zinc oxide (Al:ZnO, Ga:ZnO) [7, 5]. These are naturally occurring ENZ materials at near-infrared (NIR) and mid-infrared (MIR) regions. Furthermore, the ENZ materials used as substrates to slow down the resonance shift of metallic nanoantennas at NIR and MIR ranges [8] [5]. However, it is possible to design ENZ metamaterials operating at the working wavelength. Maas *et al.* showed that HMM exhibit ENZ nature [9]. In this thesis, I have used hyperbolic HMM as ENZ substrate to control LSPR of ND antennas.

In this work, I have numerically investigated and experimentally realized the effect of an ENZ substrate on different sizes of NDs. We used gold (Au) and titanium dioxide (TiO_2) alternative layers to create an ENZ substrate. We fabricated Au NDs

with diameters from 120 to 180 nm on glass and the designed ENZ substrate to compare the effect of ENZ substrate on resonance. The size of antenna that can resonate at visible range is quite small and slight variation in fabrication of antenna results in large spectral change. Therefore, it is important to have better control of the resonance of metallic antenna at the visible regime using ENZ metamaterial substrate.

This thesis includes five chapters. In this introduction chapter a brief overview of the thesis is presented. Second chapter explains the theory behind LSPR, ENZ and HMM. The methods such as simulation, fabrication and optical characterization of HMMs and NDs are discussed in *Chapter 3*. The numerical and experimental results are presented in *Chapter 4* and discussed in the last *Chapter 5*.

2. THEORETICAL BACKGROUND

2.1 Light and matter interaction

Light is an EM wave that interacts differently with materials depending upon type and arrangement of atoms. The free electrons of atom start to oscillate once they are excited by EM wave and the light also get affected when it propagates through the material. For instance, unpolarized incident light becomes polarized after travelling through a polarizer. The interaction of EM wave with the medium are governed by two important properties, the permittivity and the permeability.

$$\nabla^2 \mathbf{E} = \mu_0 \epsilon_0 \epsilon_r \frac{\delta^2 \mathbf{E}}{\delta t^2}, \tag{2.1}$$

where μ_0 is magnetic permeability in vacuum, ϵ_0 is electric permittivity in vacuum and $\epsilon_r = \epsilon_{material}/\epsilon_0$ is the relative permittivity of material. Comparing (2.1) to mechanical wave equation (2.2):

$$\frac{\delta^2 y}{\delta t^2} = \frac{1}{v^2} \frac{\delta^2 y}{\delta t^2} \tag{2.2}$$

and using $c^2 = 1/(\mu^2 \epsilon_0)$, where c is the speed of light, it can be shown that:

$$v^2 = \frac{1}{\mu_0 \epsilon_0} \frac{1}{\epsilon_r} = \frac{c^2}{\epsilon_r} \tag{2.3}$$

From equation (2.3) the definition of refractive index can be derived:

$$n = \frac{c}{v} = \sqrt{\epsilon_r} \tag{2.4}$$

As the formula (2.4) suggests refractive index tells the extent to which speed of light decreases when it travels through material.

The relative permittivity can be also expressed in terms of susceptibility $\chi = \chi' + i\chi''$, which is a coefficient of linear proportionality between polarization and electric field in homogeneous and isotropic media:

$$\epsilon_r = 1 + \chi' + \chi'' \tag{2.5}$$

$$n = \sqrt{1 + \chi' + \chi''}. \tag{2.6}$$

In an absorbing materials refractive index is a complex number:

$$n = n' + in''. \tag{2.7}$$

In optical range refractive index for most of the materials is in the range from 1 to 3.5.

2.2 Dispersion relation

The wavelength and speed of the light changes when it enters material with different refractive index, while the frequency remains the same:

$$w = v\frac{2\pi}{\lambda} = vk, \tag{2.8}$$

where k is the wave number. If we rewrite EM wave equation using refractive index:

$$\nabla^2\mathbf{E} = \frac{n^2}{c^2}\frac{\delta^2\mathbf{E}}{\delta t^2} \tag{2.9}$$

and substitute in equation (2.9) expression for electric field of monochromatic light wave:

$$\mathbf{E} = E_0 e^{-i(kr-wt)}, \tag{2.10}$$

we obtain a dispersion relation between wave vector and frequency

$$w^2 = \frac{c^2}{n^2}k^2 \tag{2.11}$$

or using complex notation for refractive index:

$$k = \pm\frac{w}{c}(n' + in''). \tag{2.12}$$

In equation (2.12) n' is a real number, which represents a regular refractive index, while n'' is a complex number, that represents the amplitude exponential decay along the propagation direction or absorption of the wave. Regular refractive index is defined as

$$\beta = \frac{w}{c}n' = kn'. \tag{2.13}$$

The complex part of n is called absorption coefficient:

$$\alpha = -2\frac{w}{c}n'' = -2kn''. \tag{2.14}$$

From equation (2.14) and (2.15) it follows that wavenumber k is

$$k = \pm(\beta - i\frac{\alpha}{2}) \tag{2.15}$$

2.2.1 Lorentz model

To predict optical behavior of a material we can apply Lorentz model. The response of electrons in atoms and molecules in microscopic scale will determine the overall material response to EM excitation. If rotational movement of an atom around nucleus is projected in a straight line, it is actually a harmonic oscillator trajectory. In Drude-Lorentz model each particular transition between two energy level is assigned to be a harmonic oscillator of a certain frequency. The graphical representation of an atom as harmonic oscillator is shown in **Figure 2.1**. Then, the response of an atom to EM field can be thought as a response of harmonic oscillator to a driving force. Therefore, the oscillator, whose transition frequency is the closest to light wave frequency, will be excited in the most efficient way.

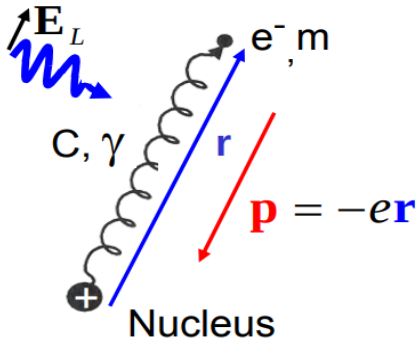

Figure 2.1 *Atomic oscillator [10]*

We can write second Newton's law for all forces acting on an electron:

$$m\mathbf{a} = \mathbf{F}_E + \mathbf{F}_{Damping} + \mathbf{F}_{Spring}, \tag{2.16}$$

where F_E is driving force of electric field, $F_{Damping}$ damping force and F_{Spring}. The

Coulomb force that attracts electron to nucleus. We now rewrite equation (2.16):

$$m\frac{d^2\mathbf{r}}{dt^2} + \mu\gamma\frac{d\mathbf{r}}{dt} + C\mathbf{r} = -e\mathbf{E}_L \exp(-iwt), \tag{2.17}$$

where γ is a decay constant, C is spring constant, E_L is local electric field experienced by a single atom. The damping force is proportional to the velocity of an electron because the fast electron will collide more. The electric dipole moment represents the extent to which electron is displaced from its equilibrium position under the effect of force applied to it. The electric dipole moment of the system is $\mathbf{p} = -e\mathbf{r}$. When substituted dipole moment in relation (2.17):

$$m\frac{d^2\mathbf{p}}{dt^2} + \mu\gamma\frac{d\mathbf{p}}{dt} + C\mathbf{p} = -e^2\mathbf{E}_L \exp(-iwt). \tag{2.18}$$

The solution of this differential equation (2.18) is of the form:

$$\mathbf{p} = \mathbf{p}_0 \exp(-iwt) \tag{2.19}$$

$$\frac{d\mathbf{p}}{dt} = -iw\mathbf{p}_0 \exp(-iwt) \tag{2.20}$$

$$\frac{d^2\mathbf{p}}{dt^2} = -w^2\mathbf{p}_0 \exp(-iwt). \tag{2.21}$$

Substituting equations (2.19-2.21) into (2.18) and cancelling exponential term, we obtain:

$$-mw^2\mathbf{p}_0 - im\gamma w\mathbf{p}_0 + C\mathbf{p}_0 = e^2\mathbf{E}_L. \tag{2.22}$$

Then, we solve for amplitude of the momentum and define $C/m = w_0^2$, w_0 being one particular fundamental frequency of transition of electron from one energy level to another:

$$\mathbf{p}_0 = \frac{e^2}{m}\frac{1}{w_0^2 - w^2 - i\gamma w}\mathbf{E}_L \tag{2.23}$$

Polarizability is then represented as coefficient of proportionality between dipole moment amplitude and electric field amplitude. Polarizability describes a response of individual atom in material:

$$\alpha(w) = \frac{e^2}{m}\frac{1}{w_0^2 - w^2 - i\gamma w}. \tag{2.24}$$

The equation (2.24) shows, the closer frequency of light to the fundamental frequency the stronger will be the response frequency. Therefore, w_0 can be named resonant

frequency. The real material consists of multiple atoms, the dipole moments of all atoms must be included in the model. In contrast to polarizability, the polarization describes dipole moment per unit volume:

$$\mathbf{P} = \frac{1}{V}\sum_j \alpha_j \mathbf{E}_L \tag{2.25}$$

$$\mathbf{P} = \frac{Ne^2}{m}\frac{1}{w_0^2 - w^2 - i\gamma w}\mathbf{E}_L \tag{2.26}$$

with N being the density number. By definition polarizability is related to susceptibility via local electric field:

$$\mathbf{P} = \epsilon_0 \chi \mathbf{E}_L. \tag{2.27}$$

Then, susceptibility as a function of frequency is:

$$\chi(w) = \frac{Ne^2}{\epsilon_0 m}\frac{1}{w_0^2 - w^2 - i\gamma w}. \tag{2.28}$$

Therefore, susceptibility is a property that describes total material response. The first fraction of this expression includes physical constants, some of which are dependent on material properties. For convenience we introduce plasma frequency $w_p^2 = Ne^2\epsilon_0 m$. Then, equation (2.28) becomes

$$\chi(w) = f\frac{w_p^2}{w_0^2 - w^2 - i\gamma w}. \tag{2.29}$$

2.2.2 Drude model

Since the electrons in metals are free there is no spring force resulting from their movement and the polarization relation (2.26) can be rewritten as:

$$\mathbf{P} = -\frac{Ne^2}{m}\frac{1}{w^2 - i\gamma w}\mathbf{E}_L. \tag{2.30}$$

Using the fundamental relation:

$$\mathbf{D} = \epsilon_0 \mathbf{E} + \mathbf{P}, \tag{2.31}$$

and inserting it into (2.30) yields:

$$\mathbf{D} = \epsilon_0(1 - \frac{w_p^2}{w^2 + i\gamma w})\mathbf{E}_L, \tag{2.32}$$

where we define plasma frequency $w_p^2 = \frac{Ne^2}{\epsilon_0 m}$. The dielectric function for free electrons in metal is shown in equation (2.32). Frequency dependent conductivity in metal is defined as:

$$\delta = \frac{\delta_0}{1 + iw\tau}. \tag{2.33}$$

2.2.3 Dielectric function of metals

The equation of motion of free electrons in metal is introduced by Newton's Second law:

$$m\frac{d^2\mathbf{r}}{dt^2} = -e\mathbf{E}. \tag{2.34}$$

Rewriting equation (2.34) with dipole moment $\mathbf{p}$:

$$m\frac{d^2\mathbf{p}}{dt^2} = e^2\mathbf{E}. \tag{2.35}$$

Substituting time-dependent dipole moment $\mathbf{p}(t) = Re\mathbf{p}(w)exp(-iwt)$:

$$-mw^2\mathbf{p}(w) = e^2\mathbf{E}(w). \tag{2.36}$$

The relative permittivity of metal is

$$\epsilon_r = 1 + \chi = 1 + \frac{N\mathbf{p}(w)}{\epsilon_0\mathbf{E}(w)} = 1 - \frac{Ne^2}{\epsilon_0 m}\frac{1}{w^2} = 1 - \frac{w_p^2}{w^2}. \tag{2.37}$$

If frequency of light is less than plasma frequency the dielectric constant is negative and response is plasmonic. In analogy to the derivation in section (2.2), we can conclude that dispersion relation of light in metal is of the form:

$$w = \sqrt{w_p^2 + c^2k^2}. \tag{2.38}$$

2.2.4 Light interaction with nanostructures

If we think of a molecule as a set of harmonic oscillators, when we excite it with light its atoms start to oscillate. Oscillating charges in turn radiate energy, called scattered light. The polarizability of nanoparticles (NPs) which are comparable with the wavelength of light is given by:

$$\Lambda = R_0\frac{\epsilon_m - \epsilon_h}{\epsilon_m + 2\epsilon_h}, \tag{2.39}$$

where ϵ_m is dielectric permittivity of metal, ϵ_h is permittivity of host material and R_0 is radius of NP. Dielectric permittivity of metal is negative. If we find such a frequency for which $\epsilon_m = -2\epsilon_h$, the denominator will drop to zero. In this case maximum polarizability or state of resonance is achieved. Therefore, the existence of surface plasmon arises from the fact that permittivity of metals is below zero. There is always a frequency at which surface plasmon is achieved. If a small particle is excited with light at resonant frequency most of the energy will be concentrated around NP hundreds times smaller than wavelength of light.

Electrons are free moving particles in metals. These free electron can be displaced collectively if they are excited by light. This displacement causes formation of excess negative and positive charges on the opposite sides of NP, which result in induced electric field within the NP itself. Under the force of secondary electric filed electrons start to oscillate between positive and negative edges. This phenomena is called surface plasmon resonance. The resonant frequency for metals can be found from Drude formula:

$$\mathbf{E}_{in} = \frac{3\epsilon_m}{\epsilon + 2\epsilon_m}\mathbf{E}_0, \tag{2.40}$$

$$\mathbf{E}_{out} = \mathbf{E}_0\left(1 - \frac{\epsilon - \epsilon_m}{\epsilon + 2\epsilon_m}\frac{a^3}{r^3}\right). \tag{2.41}$$

Equation (2.41) suggests that the strongest electric field around metal nanosphere is produced at the minimum of $|\epsilon + 2\epsilon_m|$. In other words, at a resonant frequency the electric field enhancement is at maximum:

$$Re[\epsilon(\omega)] = -2\epsilon_m. \tag{2.42}$$

2.3 Localized surface plasmon and surface plasmon polariton

The propagating surface plasmon waves on metal and dielectric interface are called plasmon polaritons. Surface plasmon excitations are bounded to and propagate along metal dielectric interface. They are also referred as surface waves. The plasmon polaritons with smaller wavelength are confined to the surface stronger.

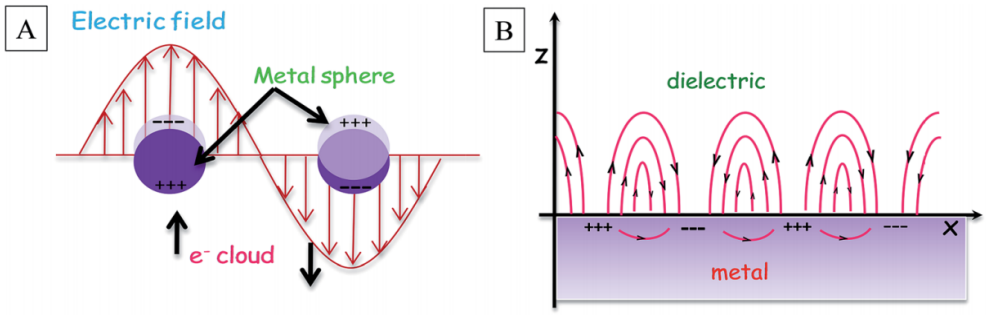

Figure 2.2 *A)Localized surface plasmon. B)Surface plasmon polariton [11].*

A NP with size much smaller than the wavelength of the excitation light, the phenomena is called localized surface plasmon.The radiation intensity and resonant wavelength of nanoantenna is determined by the property of the NP but also by the substrate. By choosing a substrate carefully one can achieve diverse behavior of light when it interacts with plasmonic antenna.

2.3.1 Epsilon-near-zero property

The ENZ material has permittivity close to zero which crosses from positive to negative region at the ENZ point. The materials with ENZ region exhibit extraordinary properties such as extremely high impedance, infinitely large wavelength within material and very small material loss [5]. Recently, naturally occurring ENZ materials are used to slow down the resonance shift. Kim *et al.* used Al:ZnO and Ga:ZnO with ENZ point in the NIR and silicon carbide (4H-SiC) with ENZ wavelength in the mid- to far-infrared range to demonstrate decreased change in resonance. In [5] nanorod antennas on naturally occurred ENZ substrate exhibit pinning effect. The pinning effect refers to the fixing of resonant wavelength for nanoantennas with varying dimension within a small interval of wavelengths. The pinning effect is observed when the structure is excited with the light at ENZ wavelength. In this thesis, I focused on artificially engineered ENZ metamaterials. The advantage of these materials is the flexibility of obtaining the ENZ wavelength by design. Hence, it allows to match ENZ wavelength with resonant wavelength of nanoantenna.

2.3.2 Hyperbolic metamaterials

Metamaterials are artificially engineered materials that harness EM waves energy for achieving an extraordinary properties of light. Because of metamaterials such

concepts as negative refraction, transformation optics, cloaking and perfect lens were introduced for the first time [12].

The HMMs are anisotropic uniaxial materials. They act as a metal along one axis and as dielectric along orthogonal direction [13]. HMMs are composed of metal-dielectric subwavelength multilayers or metal rods embedded into dielectric host. Both types are illustrated in **Figures (2.3-2.4)**. For our experiment we used the first type of HMM.

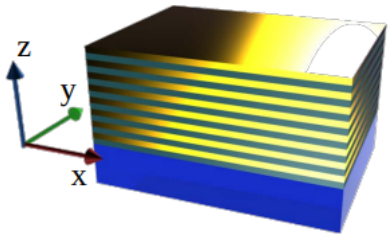

***Figure** 2.3 Multilayer HMM [10].*

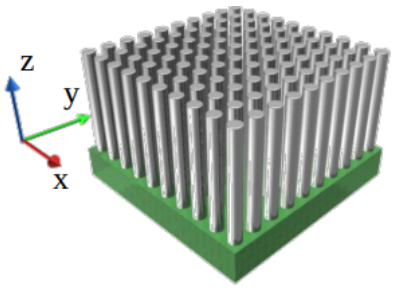

***Figure** 2.4 Nanorod HMM [10].*

To introduce EM properties of HMMs, we first determine $\epsilon_x = \epsilon_y = \epsilon_1$ and $\epsilon_z = \epsilon_2$. ϵ_1 and ϵ_2 have opposite signs. In isotropic materials permittivity is equal in all directions and frequency surface is described with sphere equation. (**Figure (2.5(a))**). In anisotropic material, permittivity along one of the axis has different sign from the other two. In this case we obtain unbound spheroid (**Figure (2.5(b))**) or hyperbolic frequency surface (**Figure (2.5(c))**).

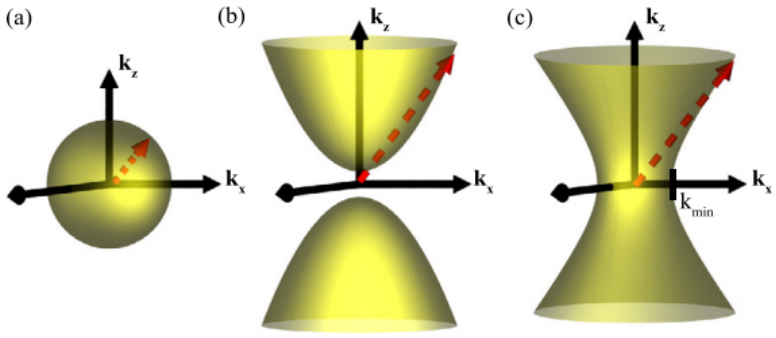

$$\frac{k_x^2+k_y^2+k_z^2}{\epsilon}=(\frac{w}{c})^2 \tag{2.43}$$

$$\frac{k_x^2+k_y^2}{|\epsilon_1|}+\frac{k_z^2}{\epsilon_2}=(\frac{w}{c})^2 \tag{2.44}$$

$$\frac{k_x^2+k_y^2}{\epsilon_1}-\frac{k_z^2}{|\epsilon_2|}=(\frac{w}{c})^2 \tag{2.45}$$

Figure 2.5 *a) Isotropic material frequency surface $\epsilon_x=\epsilon_y=\epsilon_z>0$ b) unisotropic material frequency surface $\epsilon_x=\epsilon_y>0$ and $\epsilon_z<0$ and c) $\epsilon_x=\epsilon_y<0$ and $\epsilon_z>0$ and corresponding frequency surface relations [14].*

As follows from the graph, the frequency response of HMM can grow theoretically without limit. Therefore, HMM allow the propagation of the waves with wavenumber above diffraction limit $k=w/c$. This outstanding property is used in super-resolution imaging, for example [15]. Another feature of HMMs is unbound space volume enclosed between two isofrequency surfaces which implies infinite density of photonic states. [12] High density of photonic states increases the probability of photonic processes to occur and, therefore, desirable. In reality, however, the highest value of k and number of photonic states are limited by the size of the unit cell - thickness of the smallest layer in this case.

To investigate multilayer geometry, we first describe permittivity components of the system with the help of Maxwell-Garnett approximation [12]:

$$\epsilon_1=n\epsilon_m+(1-n)\epsilon_d, \tag{2.46}$$

$$\epsilon_2=\frac{\epsilon_m\epsilon_d}{(1-n)\epsilon_m+n\epsilon_d}, \tag{2.47}$$

where ϵ_m is metallic permittivity, ϵ_d is dielectric permittivity and n is proportion of metal to the whole structure. The dispersion relation of a SPP propagating along metal-dielectric interface is:

$$k_p=\frac{w}{c}(\frac{\epsilon_d\epsilon_m}{\epsilon_d+\epsilon_m})^{\frac{1}{2}}. \tag{2.48}$$

By substituting $k_p = \sqrt{\epsilon}w/c$ we obtain effective permittivity for HMM :

$$\epsilon_{eff} = \frac{\epsilon_d \epsilon_m}{\epsilon_d + \epsilon_m}. \tag{2.49}$$

Equation (2.49) explains the relevance of HMMs for the pinning effect demonstration. The tunability of near zero point of permittivity is simply achieved by varying the thicknesses of constitutional layers. HMM's resilience occurred to be the main choice factor for the substrate material in this thesis.

3. RESEARCH METHODOLOGY

I have used numerical simulations to designs NDs as nanoantenna that has the LSPR at the ENZ wavelength of the HMM. As a first step, I obtained simulation spectrum of NDs on top of glass and later design an HMM which has ENZ response at the resonance wavelengths. The designs are experimentally realized by the fabrication of NDs on top of glass and HMM. The measured transmission results are compared. The theoretical predictions for reflection and transmission were calculated using Finite-difference time-domain *Lumerical FDTD Solutions*. Secondly, the HMM structure was fabricated using electron-beam evaporator. The nano-disk nanoantennas are fabricated using electron-beam lithography. The transmission from bare glass was measures and then from NDs on top of glass, the results of NDs were normalized to the transmission of bare glass. Similarly, for the HMM, the transmission results of NDs on top of HMM were normalized to transmission of HMM.

3.1 Simulations

Effective medium theory was used to predict the effective permittivity of the HMM. Different metal and dielectric thickness were used to design the HMM with ENZ wavelength of 680 nm. The FDTD simulation were performed to calculate the transmissions and reflection of different designs. The periodic boundary conditions along x and y axes and perfect matched layer (PML) along the z axis are defined. The plane wave source was used to excite the sample and transmission monitor was placed at λ distance from the NDs. The NDs on top glass and HMM had periodicity of 360 nm in both x and y axes. The x polarized light source was used for excitation.

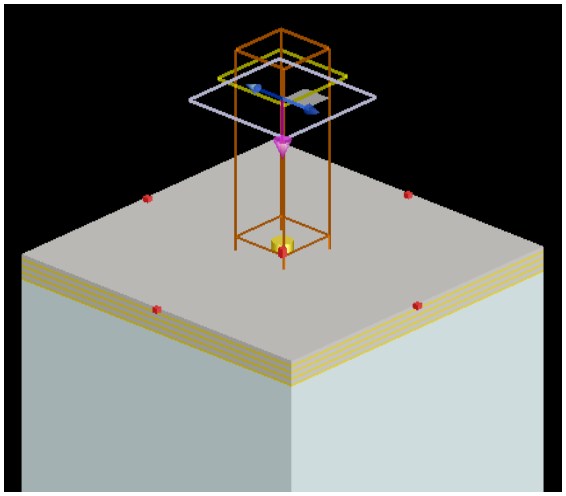

Figure 3.1 *Golden ND on Au/TiO_2 HMM substrate modelled in Lumerical FDTD*

From the simulations I have calculated LSPR of nano-antenna on top of glass. I have used polarization independent 60 nm Au NDs on glass with changing diameter from 120 to 180 nm. I have used three bilayers of 10 nm of Au and 25 nm of TiO_2 to design the HMM using effective medium theory. The effective medium theory calculation were imported to simulate the transmission results for NDs (120 to 180 nm diameters) on top HMM. The thickness of all the layers combined was 105 nm, which corresponds to the total thickness of HMM. **Figure 3.1** represents the perspective view of the structure simulated in Lumerical FDTD.

3.2 Electron beam evaporator

Electron beam evaporation is a physical vapour deposition method based on turning solid material from the source into gaseous state following by gas condensation on the target substrate. Evaporation of metal occurs in deeply evacuated chamber at a pressure less than $1 * 10^{-8}$ Pa. High voltage is applied to create a focused electron beam. The beam is directed to the crucible filled with source material. The substrate to be coated is placed over the crucible. The beam heats up the target metal until it starts to evaporate. The rate of evaporation is read by oscillation of sensitive crystal placed inside the chamber. Gaseous metal atoms rise upward, where they precipitate onto substrate forming a thin coating. During evaporation the chamber is continuously cooled down with water flow. This makes the high temperature system safe and prevents contamination of source material. It is possible to evaporate few metals in one session by changing the crucible. During sample fabrication I

evaporated three 10 nm-thick layers of gold. I also used 1 nm of titanium (Ti) to improve the adhesion of Au. **Figure 3.2** shows the schematics of e-beam evaporator.

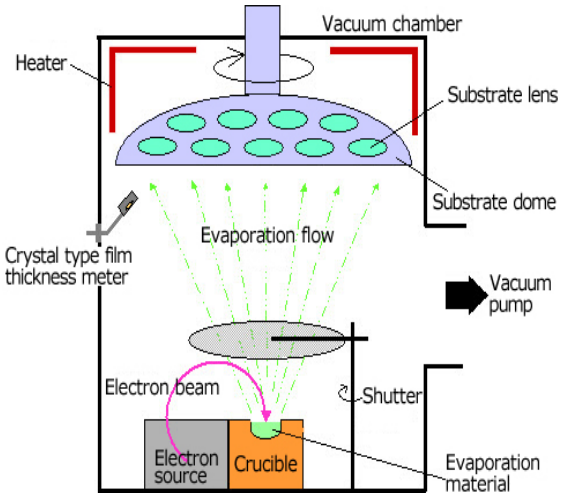

Figure 3.2 *Structure of an electron beam evaporation device [16].*

Dielectric evaporator operates in the same principal as metal e-beam evaporator. Dielectric source material is evaporated with an electron beam in evacuated chamber. Electron beam is created with a hot filament and focused at a single point with a magnetic field. In comparison to metal evaporation, when depositing dielectric, sample holder needs to be heated for better deposition quality. In addition, evaporated TiO_2 increases the pressure in the chamber, so the pressure needs to be manually stabilized throughout the deposition process with needle O_2 pump. I have deposited three 25 nm-thick layers of TiO_2.

3.3 Electron beam lithography

Electron beam lithography (EBL) is a commonly known nanopatterning technique. It utilizes the sensitivity of certain material called resist to electron flow. The substrate is first spin-coated with resist material, for example, polymethyl methacrylate (PMMA). The resist is then selectively exposed to electron beam. Sample is scanned pixel by pixel with Gaussian beam or other shaped beam. Large electron sensitive molecules of resist break down into smaller pieces. Radiated resist is then easily dissolved with a developer. Thus, the areas bombarded with electrons eliminate at this stage. PMMA is an example of positive resist. There are also negative resists. In case of negative resist the result is opposite, i.e., only regions of resist exposed to electron beam remain after developing. The amount of charge per unit area or the dose is a

parameter that plays a major role in EBL and also determines the exposure time. After developing stage leftover resist provides an access directly to the substrate. These "windows" in the resist are future patterns. The resist now serves as a stencil. The next step is deposition of target material, Au in our case. After the deposition, the rest of resist is dissolved by an appropriate solvent. Only Au deposited directly on top of the substrate persists and rest of the Au is lift off.

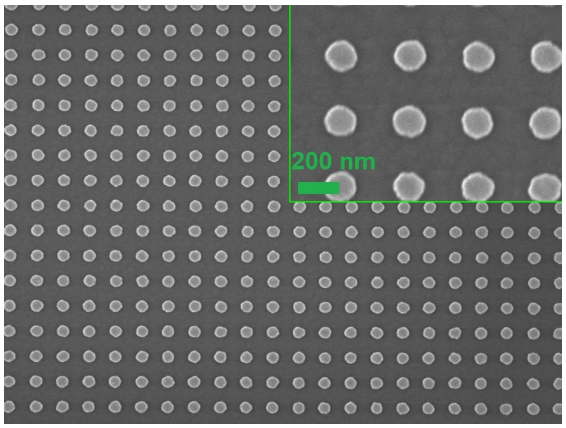

Figure 3.3 *The SEM of Au NDs fabricated on top of HMM, the scale bar is 200 nm.*

Thanks to EBL, it is possible to fabricate features with different geometries in nanoscale resolution. For this thesis we deposited Au NDs with diameters 120-180 nm on top of HMM substrate. The scanning electron microscopy (SEM) image of fabricated NDs is shown in **Figure 3.3**.

3.4 Ellipsometry

Ellipsometer allows the measurement of dielectric layer thickness and refractive index. An ellipsometer can be used to measure layers as thin as 1 nm [17]. During sample fabrication for this thesis I have used ellipsometer to verify the thickness of deposited dielectric layer. Ellipsometer consists of a laser, a polarizer, an analyzer and a compensator. The schematics of ellipsometer is depicted in **Figure 3.4**.

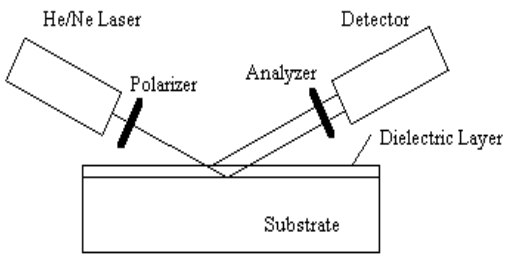

Figure 3.4 *Structure of an ellipsometer [17].*

Laser beam from the source travels through the compensator that adjusts the polarization state of a light. After reflection from the sample the polarization of light beam is changed. The change in polarization is based on the sample properties such as thickness and refractive index. The phase of the incoming light is also changed as it is transmitted through a dielectric. The analyzer only allows light of a certain polarization to pass through while the detector consists of units each sensitive to certain polarization components. Ellipsometry measures the ratio of amplitudes and phase difference of incident and reflected light. The film thickness and refractive index are then calculated using the measured parameters.

3.5 Confocal microscopy

Characterization of samples, i.e., reflection and transmission of light from fabricated structures were measured with a confocal microscopy. The schematic of an instrument is shown in **Figure 3.5**.

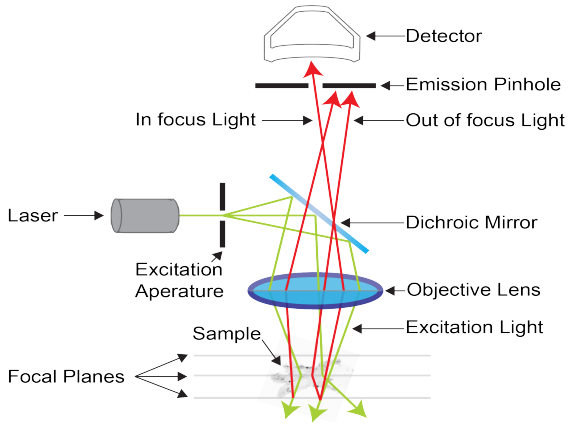

Figure 3.5 *Schematic of confocal microscope [18].*

A confocal microscope uses a laser as a source of light. Images are taken with a digital

camera trough a pinhole. The emission pinhole only lets through the light of one focal plane on which digital camera is focused. The rest of the light originated from different planes is blocked. With the help of the objective lens the light is focused on the surface of specimen. The light reflected from specimen surface is captured with digital camera or photodetector, that transforms the light signal into electrical. The laser then can be refocused to another region of specimen via an adjustable dichroic mirror. In this fashion, the laser scans the whole surface of specimen point by point. All the points are then collected into single sharp image. Slower scanning speed results in less signal-to-noise ratio and better contrast of an image. An excitation aperture can be adjusted to regulate thickness of the focal plane which is mostly defined by the wavelength of the used light.

4. RESULTS

The effective medium theory calculation and measurement results of HMM are presented in **Figure 4.1** and **Figure 4.2**, respectively. The response of HMM is characterized using transmission and reflection normalized to glass and aluminium (Al) mirror, respectively. The results show that ENZ wavelength of HMM has a crossover from transmissive to reflective materials. The effective medium theory shows that designed HMM has ENZ at 684 nm. The real part of HMM is presented in black and imaginary part in red colour in **Figure 4.1**.

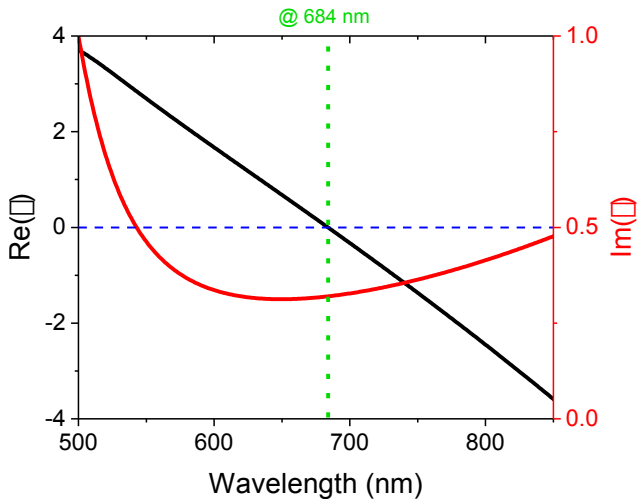

Figure 4.1 *Permittivity of the designed HMM, real (black line) and imaginary (red line) ϵ. The zero crossing point is marked.*

Similarly the transmission in black and the reflection in red are shown in **Figure 4.2**. There is a good agreement between simulation and experimental results of HMM. The zero crossing point of $Re(\epsilon)$ was chosen in such a way that it corresponds to the resonant wavelength of nanoantenna. Therefore, in this work, we used this HMM as ENZ substrate.

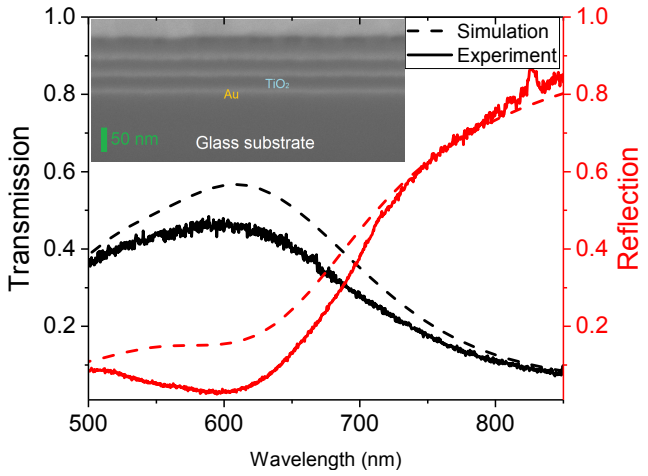

Figure 4.2 *Simulated (dashed lines) and experimental (solid lines) transmission (black lines) and reflection (red lines) curves for HMM. The inset image shows the SEM of HMM.*

The calculated effective permittivity values of HMM are imported to Lumerical FDTD where simulations are performed. For comparison we ran two simulations: 60 nm-thick Au NDs of diameters 120, 140, 160 and 180 nm are on glass and on top of HMM. The transmission results of NDs on top of glass and HMM are represented in **Figure 4.3** and **4.4**, respectively.

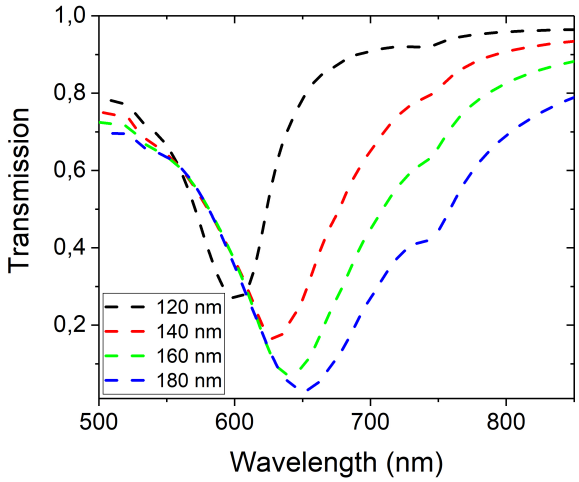

Figure 4.3 *The simulated transmission of NDs, 120 (black), 140 (red), 160 (green) and 180 nm (blue) on glass substrate.*

The total shift of the LSPR resonance for NDs with diameters from 120 to 180 nm on glass substrate is almost three times larger compare to NDs on HMM substrate.

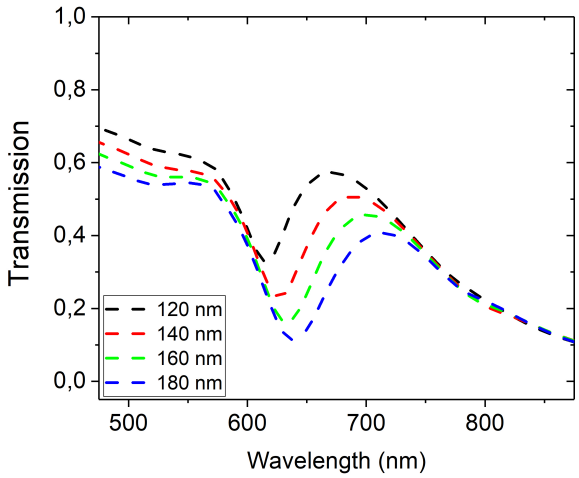

Figure 4.4 *The simulated transmission of NDs, 120 (black), 140 (red), 160 (green) and 180 nm (blue) on top of HMM.*

To experimentally realize the design the NDs were fabricated on glass and HMM and transmission measurement were performed. The normalized transmission results of glass in **Figure 4.5** shows that the resonance wavelength in transmission shifts from 628 to 678 nm.

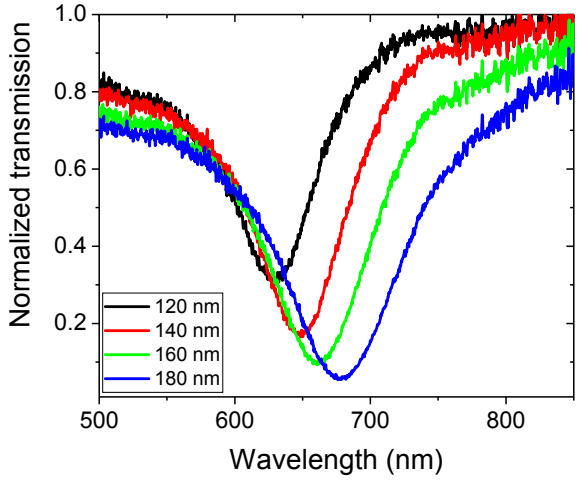

Figure 4.5 *Experimentally measured normalized transmission of fabricated NDs, 120 (black), 140 (red), 160 (green) and 180 nm (blue) on glass substrate.*

On the other hand, the ENZ substrate shifts the resonance to ENZ region of HMM. In this case the shift occurs slowly from 659 to 675 nm as shown in **Figure 4.6**.

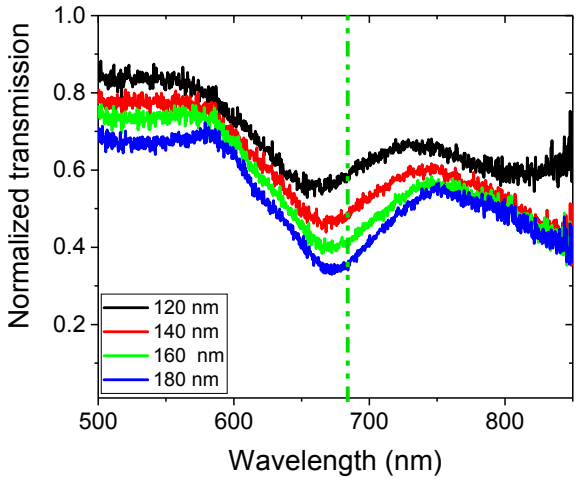

Figure 4.6 *Experimentally measured normalized transmission of fabricated NDs, 120 (black), 140 (red), 160 (green) and 180 nm (blue) on HMM substrate.*

The transmission results are the prove of the concept that by designing an ENZ substrate we can control the region of the LSPR and make it less dependent on nanoantenna size as well. Next, I made a comparison of spectral shift of LSPR on glass and HMM and plotted them versus NDs diameters (**Figure 4.7**).

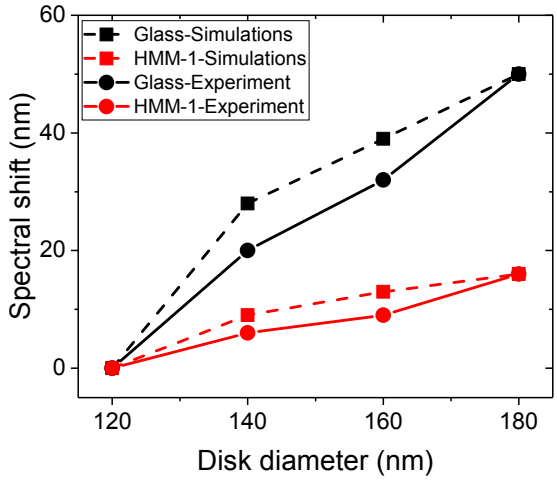

Figure 4.7 *The simulated (dashed lines) and measured (solid lines) resonance shift of NDs on top of glass (black lines) and HMM (red lines).*

The plot is a self-explanatory figure of my work that shows that the shift on HMM substrate is just 16 nm compared to 50 nm on glass. Moreover, my experimental results are in a good agreement with the simulation results.

5. CONCLUSION

In this thesis, I have demonstrated a significant change in the behavior of resonant wavelength of NDs within visible spectral range due to the presence of ENZ substrate. I have numerically investigated the slowing down of resonance shift, called pinning effect, by comparing the transmission of NDs on glass and HMM. The HMM were designed to exhibit the ENZ region in the vicinity of LSPR of ND antennas on glass. The HMMs were designed using Au and TiO_2, the most commonly used materials in plasmonics. The NDs were fabricated using standard EBL and e-beam evaporation. Transmission resonance is pinned at the wavelength 684 nm, which is ENZ wavelength of the HMM substrate. Reduced spectral shift was numerically and experimentally compared in **Figure 4.7**, where NDs diameter versus resonant wavelength are plotted. The slope of the line indicates the shift in resonance. For NDs on glass the slope is considerably steeper than for NDs on HMM. In other words, the spectral shift is larger in the absence of ENZ substrate. However, when the NDs are on HMM resonant wavelength is almost independent of their diameter. The reason of this, is the vanishing refractive index of ENZ material. Since both $Re(\epsilon)$ and $Im(\epsilon)$ of ENZ are close to zero, the refractive index, as can be seen from equation (2.4), tends to zero too. At the same time, the effective wavelength within the ENZ material grows infinitely large. Resonance frequency of a nanoantenna directly depends, among other things, on refractive index of a substrate material and effective antenna length. An increase in nanoantenna effective length is compensated by the vanishing refractive index. Hence, the resonance wavelength of NDs with different diameters remains nearly constant at ENZ wavelength. This property allows more flexibility in the design of nanostructures with NDs, since the dimension can be altered more freely without serious changes in resonant wavelength. The effective control of LSPR on tunable ENZ materials can be used for bio-sensing and enhanced emission.

BIBLIOGRAPHY

[1] W. L. Barnes, A. Dereux, and T. W. Ebbesen, "Surface plasmon subwavelength optics," 2003.

[2] S. A. Maier and H. A. Atwater, "Plasmonics: Localization and guiding of electromagnetic energy in metal/dielectric structures," 2005.

[3] E. Hao and G. C. Schatz, "Electromagnetic fields around silver nanoparticles and dimers," *Journal of Chemical Physics*, 2004.

[4] R. W. Ziolkowski, "Propagation in and scattering from a matched metamaterial having a zero index of refraction," *Physical Review E - Statistical Physics, Plasmas, Fluids, and Related Interdisciplinary Topics*, 2004.

[5] J. Kim, A. Dutta, G. V. Naik, A. J. Giles, F. J. Bezares, C. T. Ellis, J. G. Tischler, A. M. Mahmoud, H. Caglayan, O. J. Glembocki, A. V. Kildishev, J. D. Caldwell, A. Boltasseva, and N. Engheta, "Role of epsilon-near-zero substrates in the optical response of plasmonic antennas," *Optica*, 2016.

[6] J. Rensberg, Y. Zhou, S. Richter, C. Wan, S. Zhang, P. Schöppe, R. Schmidt-Grund, S. Ramanathan, F. Capasso, M. A. Kats, and C. Ronning, "Epsilon-Near-Zero Substrate Engineering for Ultrathin-Film Perfect Absorbers," *Physical Review Applied*, 2017.

[7] S. A. Schulz, A. A. Tahir, M. Z. Alam, J. Upham, I. De Leon, and R. W. Boyd, "Optical response of dipole antennas on an epsilon-near-zero substrate," *Physical Review A*, 2016.

[8] S. A. Schulz, A. A. Tahir, M. Z. Alam, J. Upham, I. De Leon, and R. W. Boyd, "Optical response of dipole antennas on an epsilon-near-zero substrate," *Physical Review A*, vol. 93, p. 063846, jun 2016.

[9] R. Maas, J. Parsons, N. Engheta, and A. Polman, "Experimental realization of an epsilon-near-zero metamaterial at visible wavelengths," *Nature Photonics*, 2013.

[10] S. V. M., "ECE 695S: Nanophotonics and Metamaterials," 2013.

[11] J. Jana, M. Ganguly, and T. Pal, "Enlightening surface plasmon resonance effect of metal nanoparticles for practical spectroscopic application," 2016.

[12] E. Shamonina, *World Scientific Handbook of Metamaterials and Plasmonics*. World Scientific, 2017.

[13] P. Shekhar, J. Atkinson, and Z. Jacob, "Hyperbolic metamaterials: fundamentals and applications," *Nano Convergence*, 2014.

[14] C. L. Cortes, W. Newman, S. Molesky, and Z. Jacob, "Quantum nanophotonics using hyperbolic metamaterials," 2012.

[15] C. Lv, W. Li, X. Jiang, and J. Cao, "Far-field super-resolution imaging with a planar hyperbolic metamaterial lens," *EPL*, 2014.

[16] "https://www.jeol.co.jp/en/science/eb.html."

[17] B. V. Zeghbroeck, "http://ecee.colorado.edu/∼bart/book/ellipsom.htm," 1997.

[18] "https://imb.uq.edu.au/facilities/microscopy/hardware-software/confocal-microscopes."